Study of the Local Structure of Molybdenum−Magnesium Binary Oxides by Means of Mo L 3 Edge XANES and UV−Vis Spectroscopy

ARTICLE *in* THE JOURNAL OF PHYSICAL CHEMISTRY · DECEMBER 1996

Impact Factor: 2.78 · DOI: 10.1021/jp9615464

8 AUTHORS, INCLUDING:

Hirofumi Aritani
Saitama Institute of Technology
40 PUBLICATIONS **703** CITATIONS

SEE PROFILE

Tsunehiro Tanaka
Kyoto University
318 PUBLICATIONS **6,007** CITATIONS

SEE PROFILE

Study of the Local Structure of Molybdenum−Magnesium Binary Oxides by Means of Mo L_3-Edge XANES and UV−Vis Spectroscopy

Hirofumi Aritani, Tsunehiro Tanaka, Takuzo Funabiki, and Satohiro Yoshida*

Division of Molecular Engineering, Faculty of Engineering, Kyoto University, Sakyo-ku, Kyoto 606-01, Japan

Kazuo Eda and Noriyuki Sotani

Department of Chemistry, Faculty of Science, Kobe University, Nada, Kobe 657, Japan

Masataka Kudo

Criminal Investigation Laboratory, Metropolitan Police Department, Chiyoda, Tokyo 100, Japan

Sadao Hasegawa

Department of Chemistry, Tokyo Gakugei University, Koganei, Tokyo 184, Japan

Received: May 29, 1996; In Final Form: August 15, 1996[⊗]

Mo L_3-edge XANES and diffuse reflectance UV−vis spectra have been recorded for structural studies of Mo−Mg binary oxides which catalyze metathesis reactions of olefins after pretreatment with H_2 at 773 K. The XANES of reference compounds revealed that the local symmetry around the Mo ion as well as the valence state affects the spectral features. From the XANES of Mo−Mg binary oxides in oxidized/reduced states, it is concluded that MoO_4 tetrahedra are the main component in the near-surface region for samples of x (Mo/(Mo + Mg)) ≤ 0.7 in the oxidized state. For samples in the reduced state, the tetrahedral species remain, but reduced Mo ions including MoO_2 species are also formed, while the MoO_2 phase is formed in the bulk phase at $x = 0.5-0.8$. In the latter samples, Mo ions are easily reduced by treatment with H_2. The active species for metathesis reactions relates to formation of the MoO_2 phase not only in the bulk but also in the near-surface region.

Introduction

It is well-known that supported molybdenum oxides catalyze metathesis reactions of olefins. So far, a variety of mechanisms and intermediates in the reaction process have been proposed for olefin metathesis.[1] Of these, a mechanism involving metal-carbenes and metallocyclobutane has been generally accepted for the heterogeneous catalysis.[2,3] As the initial step, the formation of metal-carbene species from adsorbed olefins is proposed in several studies.[4−6] It is likely that dispersed low-valent molybdenum ions play a significant role in the reaction, in particular, at the initial stage. Kazansky et al. reported[7−9] that MoO_x/SiO_2 including a Mo^{4+} monoxo-species, which is formed by pretreatment of photoreduction with CO or H_2, exhibited a high activity for olefin metathesis. Tanaka et al.[10] proposed that dispersed Mo^{4+} and/or Mo^{5+} ions participate as the active sites on MoO_x/TiO_2. However, what the active species is remained still unclear, although Zhang et al.[11] and Anpo et al.[12,13] concluded that the photoreduced Mo^{5+} dioxo-species is active for olefin metathesis.

As for MgO-supported MoO_3, it has been reported that the sample containing a relatively low amount of molybdenum is inactive for a metathesis of alkenes even after prereduction.[10] This is in marked contrast with the cases of other supports such as SiO_2, Al_2O_3, and TiO_2.[10] In the case of MgO-supported molybdena, most Mo ions are thought to be stabilized in a tetrahedral MoO_4 unit of the magnesium molybdate ($MgMoO_4$) phase formed by calcination.[14−16] The MoO_4 unit is also formed by mechanical mixing of MoO_3 and MgO,[17] indicating that Mo ions are easily diffused in MgO. Therefore, Mo ions in MgO-supported MoO_3 catalysts are naturally expected to be similar to those in Mo−Mg binary oxides.

For olefin metathesis by binary oxide catalysts including molybdenum, only a few works have been reported. In general, mixed molybdenum oxides are not active for metathesis but for oxidation of alkenes. For instance, $Bi_2O_3-MoO_3$ is known as a powerful catalyst for partial oxidation of olefins,[18] e.g., to produce unsaturated aldehydes or dienes.[19] MoO_3-SnO_2 catalysts exhibit high activity and selectivity for oxidations,[20] such as the conversion of propene to acrolein[21] and to acetone in the presence of H_2O.[22,23] A Mo−Mg binary oxide also exhibits catalytic activity for partial oxidation.[24,25] On the contrary, we found that propene metathesis takes place by MoO_3−MgO binary oxides with relatively higher Mo-loading when they are pretreated with hydrogen at 773 K.[26] It seems to be noteworthy that dispersed molybdenum ions relate to the active species for olefin metathesis. To clarify the bulk structure of Mo−Mg binary oxides, structural change by reduction with hydrogen, and generation of active species for metathesis, we have already carried out a Mo K-edge XANES/EXAFS study of MoO_3−MgO in oxidized and reduced states.[27] In the previous work, we concluded that MoO_3−MgO samples containing high amounts of molybdenum (Mo/(Mo + Mg) = 0.6−0.7) are easily reduced to form a dispersed MoO_2 superfine particle in the matrix and we deduced that this bulk species relates to the active center for metathesis.

Only a few works have been reported on the structure of Mo−Mg binary oxides so far. Mo L_3-edge XANES spectroscopy was applied to the system recently.[28] The prominent feature of the Mo L-edge XANES spectrum is the white line(s) due to 2p-4d transition.[29] Therefore, the spectrum probes the orbitals

[⊗] Abstract published in *Advance ACS Abstracts,* November 1, 1996.

S0022-3654(96)01546-8 CCC: $12.00

of 4d character participating in the Mo−O bond. The white lines of the XANES spectrum are split, corresponding to the ligand field splitting of the d orbitals.[30,31] The environmental condition of the Mo ion is sensitively reflected by the XANES spectrum.[32,33] In the study of Mo L-edge XANES spectra, Bare et al. presented that supported molybdena at low Mo content is stabilized in an octahedral MoO_6 structure on MgO, and the tetrahedral structure was formed at relatively higher contents.[28,34] This result is inconsistent with the results of the studies by UV−vis and Raman spectroscopy.[14,35]

In this paper, we describe the local structure around Mo ions of MoO_3−MgO binary oxides deduced from Mo L_3-edge XANES recorded in a total electron yield mode and UV−vis diffuse reflectance spectroscopy in order to clarify the structure in the near-surface region and formation of active species for metathesis by treatment with hydrogen.

Experimental Section

MoO_3−MgO samples were prepared as described previously.[27] In brief, the samples of Mo−Mg binary oxide, ranging in molybdenum content from 0.1 to 0.9 by atomic ratio, x (=Mo/(Mo + Mg)), were prepared by a solution-evaporation method from an aqueous AHM (ammonium heptamolybdate: $(NH_4)_6Mo_7O_{24}\cdot 4H_2O$) and $MgCl_2\cdot 6H_2O$ mixed solution, followed by drying the mixture overnight and calcination at 873 K for 3 h. Reduction of MoO_3−MgO samples was carried out by treatment with H_2 gas (100 Torr) at 773 K for 1 h and removing resultant water in a liquefied N_2 cold trap in a closed system.

The commercially available authentic samples, Na_2MoO_4, MoS_2 (Wako), PMA (phosphomolybdic acid: $H_3PMo_{12}O_{40}\cdot nH_2O$), AHM, Mo metal (Nacalai), $MoO_2(acac)_2$, $MgMoO_4$ (Mitsuwa), and MoO_2 (rare-metal), were used as references for XANES information. Other reference samples, MoO_3 and hydrogen molybdenum bronzes, were prepared in our laboratory. A MoO_3 sample was prepared by calcination of AHM at 873 K for 3 h. It has not a hexagonal but a rhombic structure. The hydrogen molybdenum bronze (H_xMoO_3)[36] samples, type I ($0.21 < x < 0.40$)[37] and type II ($0.85 < x < 1.04$), were prepared by a method as reported by Sotani et al.[38] The bulk structures of these reference samples were analyzed by powder X-ray diffraction.

The Mo L_3-edge XANES data were collected at a facility of the BL-7A station of the soft X-ray beam line at UVSOR, at the Institute for Molecular Science, Okazaki, Japan, with a ring energy of 750 MeV and stored current of 100−200 mA. Synchrotron radiation from the wiggler operated at 4 T in the bending magnet was used. Each sample was prepared for measurement by pasting with hexane and was then spread on a beryllium−copper dynode, which was attached to the first stage of an electron multiplier placed in a vacuum chamber. After the chamber had been evacuated ($<1.0 \times 10^{-7}$ Torr), the spectrum was recorded in a total electron yield mode at room temperature, using a Ge(111) two-crystal monochromator. The beam size at the sample was 1.0×5.0 mm^2. At the Mo L_3-edge (2.52 keV), energy resolution was about 0.3 eV. In the measurement, not only LMM Auger electrons but also low-energy secondary electrons constitute a significant fraction of the spectra in the total electron yield mode.[39] The penetration range of the spectra is possibly several hundred angstroms into the bulk. Thus, the spectra reflect the structure of the samples in the "near-surface region". The photon energy was calibrated by the Mo L_3-edge of a Mo metal sample (2520.63 eV), and this energy is set as a standard reference energy. The TEY signal (I) of the samples was normalized to the signal (I_0) without the Mo sample ($\mu = I/I_0$). μ was normalized to the post-edge intensity (at +27 eV from the edge position) to adjust the height around the post-edge region for each spectrum.

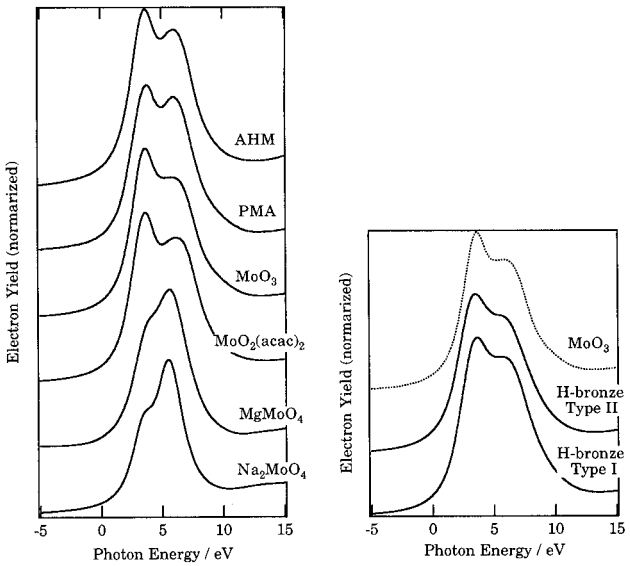

Figure 1. Mo L_3-edge XANES spectra of reference compounds including Mo^{6+} ions.

UV−vis spectra of powdered samples were recorded in a diffuse reflectance mode, with a Perkin-Elmer LAMBDA-19 spectrometer at room temperature, using an *in situ* cell for mounting the powdered samples.

Results and Discussion

(1) Mo L_3-Edge XANES of Reference Compounds. The origin of Mo L_3-edge XANES is mostly the electron transition from a core level, $2p_{3/2}$, to a vacant 4d state. Teo and Lee showed that the contribution of p−s transition to L_3-edge absorption spectra is about 50 times less than that of p−d transition.[29] Figure 1 shows the Mo L_3-edge XANES spectra of reference compounds with the $Mo^{6+}(d^0)$ ion, except for MoO_2, MoS_2, and Mo metal. In the case of $MgMoO_4$ and Na_2MoO_4 having tetrahedral (MoO_4) units, the two white lines of each XANES spectrum are attributed to the electron transition from $2p_{3/2}$ to split 4d states, i.e., t_2 (d_{xy}, d_{xz}, and d_{yz}) and e ($d_{x^2-y^2}$ and d_{z^2}). For these samples, the white line in higher energy side is more intense (peak height) than that at the lower one. On the other hand, for the XANES spectra of MoO_3, $MoO_2(acac)_2$, AHM, and PMA having octahedral MoO_6 units, the two white lines are due to the electron transition from $2p_{3/2}$ to t_{2g} (d_{xy}, d_{xz}, and d_{yz}) and e_g ($d_{x^2-y^2}$ and d_{z^2}) of the 4d state of atomic orbitals. In these samples, it is clear that the white line on the higher energy side is less intense than that on the lower one. It is quite different from the case of MoO_4 tetrahedra due to the difference of the transition cross sections in the molecular orbital of Mo(4d)−O(2p) between tetrahedral and octahedral molybdena; that is, the intensity is t_{2g}:e_g = 3:2 for the octahedron and e:t_2 = 2:3 for the tetrahedron.

To clarify the ligand field splitting of the final state 4d orbitals by splitting of L-edge XANES, a second-derivative spectrum is often used.[28,30,31,33] The second derivatives of XANES spectra exhibit the splitting more clearly, and the energy gap reflects the d orbital splitting directly, as shown in Figure 2. The energy gaps between the two white lines were evaluated and are listed in Table 1. For those samples having MoO_4 tetrahedra, the energy gap is 2.2−2.3 eV, while for MoO_3, having distorted MoO_6 octahedra, the gap is 3.3 eV. The values are the same as those reported by Bare et al.,[28] who recorded the XANES spectra in a fluorescence yield mode. XANES spectra of MoO_2-

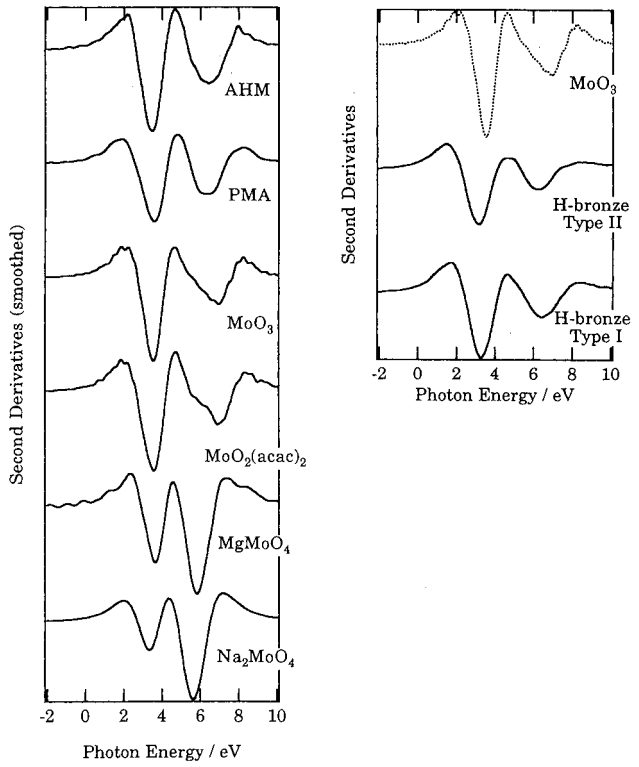

Figure 2. Second derivatives of Mo L_3-edge XANES spectra of reference compounds including Mo^{6+} ions.

TABLE 1: Energy Gap between the Two White Lines (Obtained by Second Derivatives of XANES Spectra)

sample	local structure	peak energy[a] (eV)		d orbital splitting (eV)
Na_2MoO_4	T_d	3.5	5.7	2.4
$MgMoO_4$	T_d	3.6	5.8	2.2
AHM[b]	O_h (nearly C_{2v})	3.5	6.4	2.9
PMA[c]	O_h (nearly C_{2v})	3.6	6.4	2.8
MoO_3	O_h (distorted)	3.6	7.0	3.4
$MoO_2(acac)_2$	O_h (distorted)	3.6	6.9	3.3
type I[d]	O_h[e]	3.3	6.4	3.1
type II[d]	O_h[e]	3.2	6.3	3.1
MoO_2	O_h	1.4	3.8	2.4
MoS_2	D_{3h}	1.7		
Mo (metal)	⟨*bcc*⟩	0.0		

[a] Energy offset is taken to be 2520.6 eV. [b] Ammonium heptamolybdate: $(NH_4)_6Mo_7O_{24}\cdot 4H_2O$. [c] Phosphomolybdic acid: $P_2O_5\cdot 24MoO_3\cdot xH_2O$. [d] Hydrogen molybdenum bronze (H_xMoO_3) sample. [e] Axially symmetric. (The distances of the six Mo−O bonds are different from each other.)

$(acac)_2$, AHM, and PMA comprising MoO_6 units are shown in Figure 1. For MoO_3 and $MoO_2(acac)$, with a distorted O_h structure, the splitting gaps are 3.3−3.4 eV, while, for AHM and PMA having a Mo polyanion structure with almost O_h but nearly C_{2v} symmetry, the energy gaps between the two peaks are around 2.9 eV. In the former two compounds, oxygen ligands on an equatorial plane are located at apexes of an almost regular square. This results in the inability of the e_g $d_{x^2-y^2}$ orbitals to be raised, resulting in large energy gaps.

In the case of the polyanion structure such as the $(Mo_7O_{24})^{6-}$ ion in AHM, distorting Mo ions interact with the neighboring Mo ions so that the bond strengths of Mo−O are weakened, with the result that the molecular orbitals corresponding to Mo−O_6 are more spread and the d band is tighter than that of completely O_h symmetric octahedra.[40] Therefore, the energy gap between t_{2g} and e_g is smaller than that for MoO_3 and/or $MoO_2(acac)_2$, which have slightly distorted MoO_6 octahedra, but the lengths of the six Mo−O bonds are almost similar to those of MoO_3. This tendency of distortion effect is also reflected in the HOMO−LUMO gap, which relates to UV−vis spectroscopy directly,[40] as discussed in a later section. As long as the discussion is limited to the local symmetry, the local structure of the $(PMo_{12}O_{40})^{3-}$ anion in PMA is almost similar to that of the $(Mo_7O_{24})^{6-}$ ion in AHM, reported by ^{95}Mo-NMR studies.[41,42] Thus, the splitting of PMA is assigned as the same as that of AHM.

We investigated the L_3-edge XANES of Mo−Mg binary oxides in the reduced state as described in a later section. Thus, information on the local structure of compounds including reduced Mo ions is necessary for the discussion of the reduction effect. Hydrogen molybdenum bronze (H-bronze) and MoO_2 samples are available for reference to obtain spectral information on MoO_6 octahedra with reduced Mo ions. In the case of H-bronzes, MoO_6 octahedra of $(MoO_6)_n$ sheets cause minor rearrangements in the Mo−O framework by insertion of hydrogen into MoO_3 interlayers.[43,44] As a result, the H-bronze samples have axially symmetric MoO_6 units and six Mo−O bonds, whose distances are almost the same as those of MoO_3.[45] Hydrogen atoms are intercalated into the $(MoO_6)_n$ layers and stabilized by linking to oxygen atoms, resulting in OH or OH_2 groups located between the intra- and interlayers.[45] In this manner, hydrogen atoms act as a structural change in MoO_6 octahedra; however, it is naturally accepted that formation of reduced Mo ions such as Mo^{5+} and/or Mo^{4+} is brought about by insertion of hydrogen atoms. The H-bronze shows distinct phases, called type I-IV, depending on the number of intercalated hydrogen atoms. We recorded the L_3-edge XANES spectra of the H-bronze samples of types I and II. For these samples, $H_{0.21}MoO_3$ of type I and $H_{0.91}MoO_3$ of type II were observed in the bulk phase.[45,46] The L_3-edge XANES spectra of H-bronze samples and their second derivatives are shown in Figures 1 and 2. For these samples, the number of hydrogen atoms of type I is smaller than of type II, as mentioned above.[45] The peaks of XANES over H-bronzes are positioned at lower energy than those of other samples with Mo^{6+} octahedra, e.g., MoO_3, indicating that reduced Mo ions exist in H-bronzes. Thus, it is clearly shown that intercalated hydrogen atoms in H-bronzes bring about not only formation of axially symmetric MoO_6 octahedra but also reduction of Mo ions. For these spectra, the peak at the lower energy side is positioned at 3.2−3.3 eV, which is independent of the amount of hydrogen. Furthermore, the energy gap of the splitting is also similar in these spectra. These results show that intercalation of hydrogen atoms brings about the formation of axially symmetric MoO_6 octahedra in $(MoO_6)_n$ sheets even for $x \geq 0.3$ (type I) in H_xMoO_3, and increasing the amount of hydrogen does not cause more reduction of surface Mo ions but affects the bulk Mo ions. The results of type II are that hydrogen atoms intercalate into $(MoO_6)_n$ sheets similarly to those of type I and elongate the lattice spacings between these sheets.[45,47] When the bronzes are assumed to have only a Mo^{6+} ion, the energy gap between the two white lines is expected to be larger than that of MoO_3 and the white line at the higher energy side should be narrower, because the MoO_6 unit in H-bronze is closer to a regular octahedron than that in MoO_3. However, the energy gaps of the splitting of H-bronzes are smaller than that of MoO_3. This suggests that the reduction of Mo ions results in a decrease of the energy gap between t_{2g} and e_g in the 4d state of Mo. This is also discussed in the analysis of MoO_2 XANES, below.

The $Mo^{4+}(d^2)$ ions in MoO_2 exist in an almost symmetric MoO_6 O_h structure. For the local structure of MoO_2 with an orthorhombic system, the 3-fold-degenerate t_{2g} manifold of

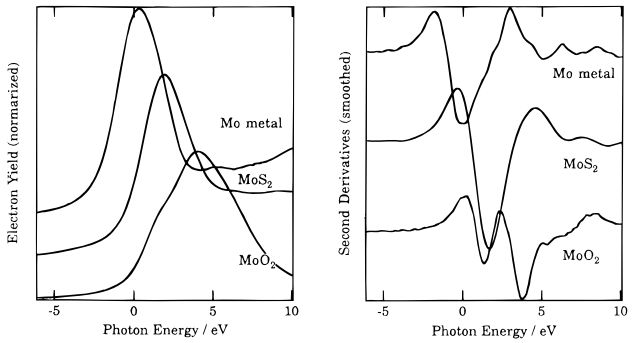

Figure 3. Mo L_3-edge XANES spectra (left) and their second derivatives (right) of Mo, MoS_2, and MoO_2.

MoO_6 octahedral symmetry is split into a more stable $d_{||}$ (d_{xy}) orbital and two $d_\perp$ (d_{xz} and d_{yz}) orbitals. The $d_\perp$ orbitals overlap the p_π orbitals of O^{2-} ions, which have three coplanar Mo near neighbors, and form $Mo(d_\perp)-O(p_\pi)-Mo(d_\perp)$ bonding, whose interactions bring about a quasidegenerate pair of π^* bands.[36] Studies of He-I photoelectron spectroscopy concluded that the 4d electron of Mo^{4+} participates in the π^* bands.[48] Therefore, in MoO_2, a pair of Mo 4d electrons in the t_{2g} state occupy molecular orbitals of $Mo(d_\perp)-O(p_\pi)$ and the orbitals in the e_g state are vacant. The energy gap between t_{2g} and e_g in MoO_2 having Mo^{4+} ions should be smaller than that of the sample having Mo^{6+} ions, because of the lesser effect of perturbation by the ligand field of the six O ions. In the XANES spectrum of MoO_2, shown in Figure 3, a shoulder peak at 1.4 eV due to an electron transition to the π^* band is seen. The intensity of this peak is less than that of the samples including Mo^{6+} ions, because of the decrease in transition cross sections. The broad peak maximized at 3.8 eV is due to the transition to the e_g state. The splitting of these peaks can be clearly seen in the second-derivative spectrum. The 2.4 eV energy gap is much smaller than that of MoO_3, although the Mo ions in MoO_2 exist in symmetric MoO_6 octahedra. This result strongly explains that the reduction of Mo ions brings about the condensation of a total 4d state, and it reflects the L_3-edge XANES spectra directly. The reduction of Mo ions from Mo^{6+} gives the lower absorption edge and narrower splitting of the energy gap, regardless of the symmetry of the MoO_6 octahedra.

In the case of MoS_2 having trigonal prismatic MoS_6 octahedra, the $Mo^{4+}(4d^2)$ configuration lies at the top of the $S^{2-}(3p^6)$ band. The Mo−Mo 4d electron bonding is formed as zigzag chains, and the octahedral site allows Mo−Mo bonding only with the three t_2 orbitals. These orbitals bring about the electron conduction band, as shown by a molecular orbital study by Hughbanks et al.[49] Therefore, the electron transition from 2p to 4d is assigned to an interatomic-like transition of a d−d band that is delocalized in the Mo 4d state but not to an atomic-like transition like that of MoO_2. As shown in the XANES spectrum of MoS_2 (Figure 3), the spectrum does not have split bands but shows only a single band. This feature of the spectrum is also seen in the case of Mo metal. In MoS_2, the peak energy of the XANES spectrum is 2.4 eV, which is located between the two peaks of MoO_2. It is possibly supported that the XANES of MoS_2 at the L_3-edge is due to the electron conduction band formed by the interatomic transition, and the ligand field reflects the XANES directly.

(2) Mo L_3-Edge XANES of MoO_3-MgO. We discussed the bulk structure of Mo−Mg binary oxides on the basis of the XRD and Mo K-edge XAFS in a previous report.[27] In brief, it is concluded that α-$MgMoO_4$ and MgO phases exist in the samples of low Mo ratio less than $x \leq 0.5$, and the phases including the Mo polyanion such as $Mg_2Mo_3O_{11}$ are stabilized

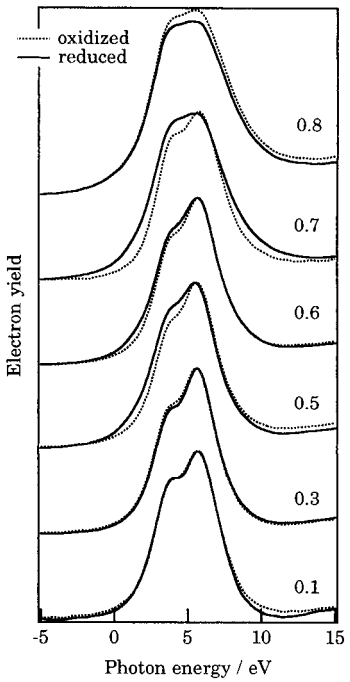

Figure 4. Mo L_3-edge XANES spectra of MoO_3-MgO in oxidized (dotted line) and reduced (solid line) states.

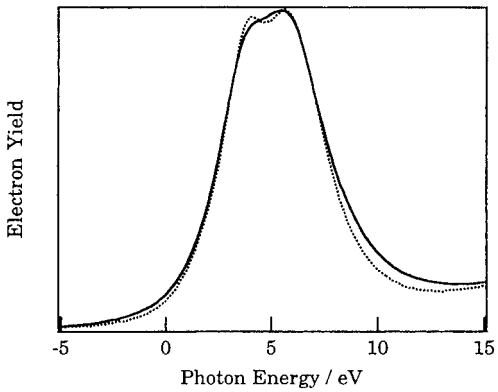

Figure 5. Mo L_3-edge XANES spectra of a reduced sample of $x = 0.7$ (solid line) and a superposed spectra (dotted line) obtained by a mixture of MoO_2 (multiplied by 20%), $MgMoO_4$ (45%), and AHM (35%).

in the samples of higher ratio. It is important to investigate the local structure in the near-surface region and clarify the relationship between bulk and surface structures for the discussion of catalytic behavior.

In this study, we recorded the Mo L_3-edge XANES spectra in a total electron yield mode. These spectra reflect the state of Mo ions in the near-surface region, as described in the Experimental Section. The spectra of MoO_3-MgO are shown in Figure 4. The dotted lines are the spectra of the samples prior to the hydrogen treatment (oxidized state), and the solid lines are the spectra after the treatment at 773 K (reduced state).

For the samples of low Mo ratio less than $x \leq 0.5$, each spectrum is similar to that of $MgMoO_4$ or Na_2MoO_4. The values of the energy gap between the two white lines determined by the second derivatives of the XANES spectrum (Figure 6) are shown in Table 2 (oxidized state) and Table 3 (reduced state). The values in these samples are 2.1−2.2 eV, and these are close to those of $MgMoO_4$ and Na_2MoO_4. These results indicate that the local structure around surface Mo ions is stabilized as MoO_4 tetrahedra, as in the bulk. However, the XANES spectra of these samples are partly different from that of $MgMoO_4$. For the samples of $x = 0.1$ and 0.3, the relative intensities (peak

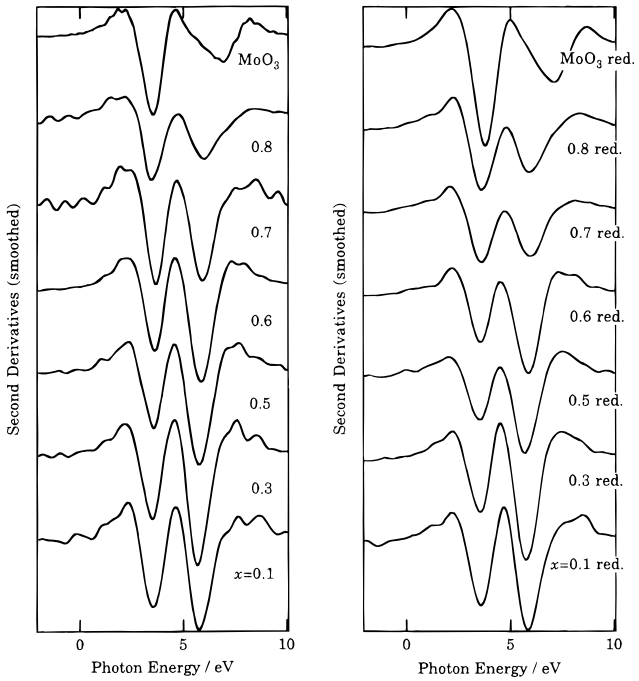

Figure 6. Second derivatives of Mo L_3-edge XANES spectra of MoO_3−MgO in oxidized (left) and reduced (right) states.

TABLE 2: Energy Gap between the Two White Lines of MoO_3−MgO

Mo ratio	peak energy (eV)		d orbital splitting (eV)
0.8	3.4	6.0	2.6
0.7	3.7	5.9	2.2
0.6	3.7	5.9	2.2
0.5	3.6	5.7	2.1
0.3	3.5	5.7	2.2
0.1	3.6	5.7	2.1

TABLE 3: Energy Gap between the Two White Lines of Reduced MoO_3−MgO

Mo ratio	peak energy (eV)		d orbital splitting (eV)
MoO_3 red.	3.8	7.1	3.3
0.8 red.	3.7	5.9	2.2
0.7 red.	3.7	6.0	2.3
0.6 red.	3.6	5.9	2.3
0.5 red.	3.5	5.7	2.2
0.3 red.	3.6	5.7	2.1
0.1 red.	3.6	5.7	2.2

height) of the two white lines are not the same as that of $MgMoO_4$, but the white line at the lower energy side is more intense than that of $MgMoO_4$. This result suggests that MoO_6 octahedra exist in the near-surface region. In $x = 0.5$, the XANES spectrum is quite similar to that of $MgMoO_4$, indicating that the Mo ions exist in a tetrahedra like that of $MgMoO_4$ not only in the bulk phase but also in the near-surface region.

For the samples of $x = 0.1$ and 0.3, the XANES spectra in the oxidized state are almost the same as those in the reduced state. This result shows that no effect by H_2 treatment is brought about for the surface Mo ions in these samples. On the other hand, changes of the XANES spectra were observed by treatment with H_2 in the samples of $x \geq 0.5$. Thus, we will discuss the XANES spectra of the oxidized samples of $x \geq 0.5$ first.

The XANES spectra of $x = 0.6$ and 0.7 have a different feature from that of $x = 0.8$. For the samples of $x = 0.6$ and 0.7, the spectra have a feature similar to that of $x = 0.5$. The energy gaps between the white lines are 2.2 eV, and this value is the same as that of $MgMoO_4$. These results show that the MoO_4 tetrahedron is a main component in the near-surface region. However, in the case of the spectrum of $x = 0.7$, the white line at the lower energy side is more intense than that of $MgMoO_4$, whose feature is the same as that of $x \leq 0.3$, indicating that MoO_6 octahedra are stabilized partly in the near-surface region. For the sample of $x = 0.8$, a white line at the higher energy side has a broad band, which is characteristic of those of the reference samples with MoO_6 octahedra such as AHM and MoO_3, indicating that the surface Mo species exist as octahedra mainly. The energy gap between the white lines is 2.6 eV. This value is close to AHM and PMA rather than MoO_3 and $MoO_2(acac)_2$. Thus, distorted octahedra having a polyanion-like structure are mainly exposed in the near-surface region.

These results lead to a conclusion that the local structure of Mo ions in the near-surface region is not necessarily the same as that in the bulk phase. Bare et al. reported an L-edge XANES study of MgO-supported MoO_3 measured in a fluorescence mode in a recent paper.[28] They concluded definitely by means of XANES spectra and their second derivatives that Mo-ion species on MgO are stabilized as octahedra in the samples of loading amount less than 15 wt % MoO_3 and that tetrahedra exist in the samples of higher loading. The present study reveals that the samples of lower Mo ratio less than $x = 0.3$ (51.7 wt % MoO_3) have an octahedral species. The previous study of these samples showed that MgO and $MgMoO_4$ phases coexist in the bulk, and Mo species are almost all MoO_4 tetrahedra, as mentioned above.[27] From the results of Bare et al. and ours, it is proposed that octahedral species in the surface or near-surface region are stabilized by the existence of the MgO phase and/or the coexistence of $MgMoO_4$ and MgO phases in the bulk. In addition, it is concluded by the present study that the generation of octahedral species in the near-surface region occurs in the samples with a higher Mo content ($x \geq 0.7$) than that in the bulk phase ($x \geq 0.6$).

By treatment with H_2, XANES spectra of $x \geq 0.5$ samples are changed. In these samples, the edge energy of each XANES spectrum becomes lower than that in oxidized samples. This strongly suggests that Mo ions are reduced by treatment with H_2. It is noteworthy that the sample of $x = 0.5$ is also reduced partly by the treatment, and the spectrum becomes similar to those of H-bronze samples. The sample in the oxidized state has only the $MgMoO_4$ phase in both bulk and surface layers, as mentioned above. For the sample of $x = 0.6$, the change in the spectrum by the treatment is almost similar to that of $x = 0.5$.

On the other hand, the samples of $x = 0.7$ and 0.8 showed a different change in the XANES spectra from those of $x \leq 0.6$ by the H_2 treatment. In the XANES spectra of $x = 0.7$, the two white lines are not clearly split, and the edge of a white line at the lower energy side shifts more than that for the sample of $x = 0.6$. This phenomenon was not observed for MoO_3. From these results, it is concluded that surface Mo ions of $x = 0.7-0.8$ samples are easily reduced by the treatment to bring about reduced ions, e.g., Mo^{5+} and/or Mo^{4+}. In fact, the XANES spectrum of $x = 0.7$ in the reduced state is able to fit the superposition of the spectra of $MgMoO_4$ (multiplied by 45%), AHM (35%), and MoO_2 (20%), as shown in Figure 5, indicating that the reduced ions including a MoO_2 phase are formed in the near-surface region by H_2 treatment. In the XANES spectrum of these reduced samples, the values of the energy gap between the white lines are 2.2−2.3 eV, suggesting that Mo^{6+} tetrahedral species still remain in the reduced state. The previous study on Mo K-edge XAFS revealed the formation

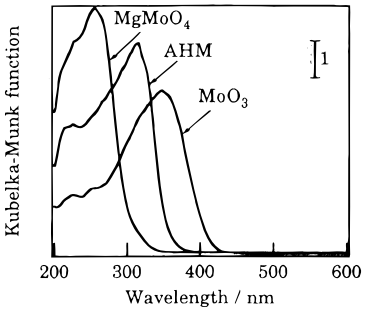

Figure 7. UV−vis reflectance spectra of Mo^{6+} reference compounds.

of MoO_2 as a definite phase.[27] Therefore, it is concluded that the Mo ions of the samples at around $x = 0.7$ are easily reduced to form a MoO_2 phase by H_2 treatment more intense in the bulk than in the near-surface region, and the surface Mo ions are stabilized as a coexistence of Mo^{6+} tetrahedra and octahedra and MoO_2. It should be mentioned that the reduced samples of around $x = 0.7$ exhibit catalytic activity for olefin metathesis.[26] The present results suggest the generation of the activity is related to the formation of reduced Mo ions in the MoO_2 phase.

(3) Diffuse Reflectance UV−vis Spectroscopy. To obtain more information about the reduced state of surface Mo ions, UV−vis spectroscopy was applied in a diffuse reflectance mode. The structural study by UV−vis spectra has already been reported, and the assignment of the bands has been done.[50−52] In the present work, MoO_3, $MgMoO_4$, AHM, and MoO_2 are used for reference compounds for the discussion about the local structure of Mo ions.

The energy of electron transitions depends on the ligand field symmetry surrounding the Mo center. For oxygen ligands, a more energetic transition is expected for a tetrahedral Mo^{6+} than for an octahedral one.[53] The spectra of the reference compounds with Mo^{6+} ions are shown in Figure 7. The spectrum of $MgMoO_4$ shows an absorption maximum at 256 nm, which is due to the ligand−metal charge transfer (LMCT) of $O^{2-} \rightarrow Mo^{6+}(d^0)$ of $(MoO_4)^{2-}$ in T_d symmetry.[35,50,51] For the samples having Mo^{6+} octahedra, the band was centered at 315 nm in AHM and at 348 nm in MoO_3, which are also due to the LMCT of $O^{2-} \rightarrow Mo^{6+}$ of MoO_6 octahedra. By distortion of the MoO_6 structure, the LMCT band shifts to a shorter wavelength. In addition, the threshold energy also reflects the local structure as reported by Weber et al.;[54] that is, the energy of polymolybdate samples becomes lower with the aggregation of MoO_6 units. This is good information for distinguishing the local structure.

The spectra of Mo−Mg binary oxides in the oxidized state are shown in Figure 8 (left side). In the case of the oxidized samples of $x \leq 0.5$, each spectrum clearly exhibits an absorption band centered at around 250 nm, indicating that Mo ions exist as T_d structures with Mo^{6+}. For instance, the spectrum of the $x = 0.5$ sample is similar to that of $MgMoO_4$ as a whole. Thus, Mo ions are stabilized as only Mo^{6+} tetrahedra. However, the spectra of the samples of $x \leq 0.3$ are different from that of $x = 0.5$. The threshold energy of $x \leq 0.3$ is higher than that of $x = 0.5$, indicating the coexistence of octahedral and tetrahedral species. This result is in accordance with that of the L_3-edge XAFS study but not with the studies of Mo K-edge XAFS and XRD.[27] Therefore, it is supported that MoO_4 tetrahedra are formed in the bulk phase, and the octahedral species are present only partly in near-surface region. This implies that the information obtained by diffuse reflectance UV−vis spectra is more sensitive to the surface structure than that of Mo K-edge XAFS spectra.

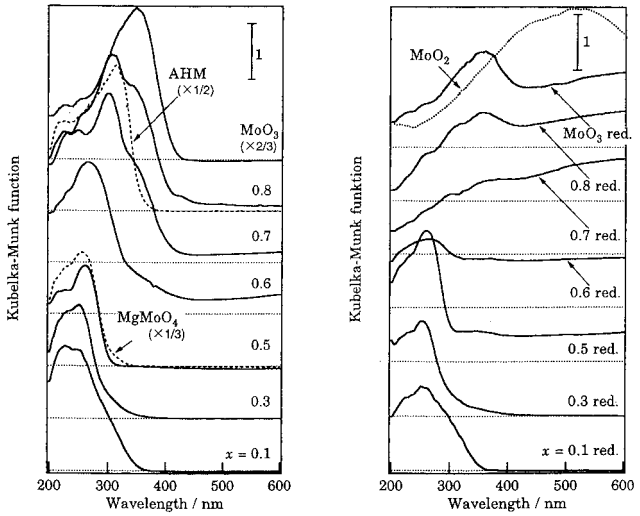

Figure 8. UV−vis reflectance spectra of MoO_3−MgO in oxidized (left) and reduced (right) states.

In the case of the sample of $x = 0.6$, the threshold energy of the spectrum is lower than that of $MgMoO_4$, and the absorption maximum is seen at 264 nm. These features are the same as those of $x \leq 0.3$, indicating that Mo ions are present as a mixture of octahedra and tetrahedra. With respect to the XAFS studies in the sample, octahedral structures of Mo ions are less observed in the near-surface region and are investigated more in the bulk. Therefore, the octahedra analyzed by UV−vis spectroscopy are formed in the bulk phase. It is explained that the diffuse reflectance UV−vis spectra include information on the bulk more than the L_3-edge XANES spectra in a total electron yield mode. Therefore, the surface sensitivity of these spectra, in the present case, is in the following order: L_3-edge XANES in a total electron yield mode > diffuse reflectance UV−vis > K-edge XAFS in a transmission mode.

On the other hand, the spectra of $x \geq 0.7$ have a large and narrow band maximized at 290 nm and a smaller band in a shoulder peak at around 345 nm. The wavelength of the absorption maximum at 290 nm is close to that of AHM having distorted octahedra, indicating that the structure around Mo ions is distorted MoO_6 octahedra like a polyanion. In a similar manner, the smaller band at around 345 nm is due to the MoO_6 octahedra in a MoO_3 phase. This peak is more intense with increasing the Mo content. As for L_3-edge XANES spectroscopy, it is concluded that the sample of $x = 0.7$ has MoO_6 octahedra as a minor component, while the result of the UV−vis spectrum shows that the octahedra as a polyanion structure are formed as a main component. Therefore, this shows that the concentration of MoO_6 octahedra is lower in the near-surface region than in the bulk.

The spectra of reduced samples treated with H_2 at 773 K are also shown in Figure 8 (right side). For the samples of $x \leq 0.3$, a band is seen at 260 nm, which corresponds to MoO_4 tetrahedra with Mo^{6+} ions. For the samples of $x = 0.1$, the spectrum is identical with the unreduced one, i.e., stabilized as a coexistence of tetrahedra mainly and octahedra partly. Thus, it is suggested that the structure of surface Mo ions is less changed by H_2 treatment. At a relatively higher Mo ratio of $x \geq 0.5$, a broad band at a wavelength longer than 320 nm is exhibited, and the absorption becomes more intense with an increase in Mo ratio. The absorption of wavelength between 400 and 800 nm is due to reduced Mo ions such as $Mo^{5+}(d^1)$ and/or $Mo^{4+}(d^2)$.[51] This indicates that reduced Mo ions are formed by treatment with H_2. The band at around 250 nm is less intense in $x = 0.6$ than in $x \leq 0.5$, and this band almost

disappears for the higher Mo content in $x \leq 0.7$. The relative intensity of the absorption at 350 nm, which is due to the Mo^{6+} octahedra in MoO_3, increases with an increase of Mo content, and this is also seen clearly for the sample of H_2-treated MoO_3. In the reduced samples at around $x = 0.7$, this band can be seen indefinitely. Thus, the Mo^{6+} octahedra in oxidized samples are reduced by H_2 treatment at 773 K to form other structures having reduced Mo ions. Therefore, results the treatment is more effective for octahedra in MoO_3 than for polyanion structure in coexistence with tetrahedra. For the broad band at a longer wavelength than 450 nm, deeply reduced Mo ions such as MoO_2 species are likely. For MoO_2, which has slightly distorted O_h symmetry around the Mo^{4+} ion, the absorption is maximized at 480 nm due to $T_{1g} \rightarrow T_{2g}$ of $Mo^{4+}(d^2)$.[51] On the other hand, the absorption band due to MoO_2 is seen less in the spectrum of H_2-treated MoO_3. Thus, bulk MoO_3 is not reduced enough to produce MoO_2 species. As discussed above, the formation of the MoO_2 phase by treatment with H_2 at 773 K is clearly shown in the bulk phase for the samples at around $x = 0.7$ by Mo K-edge XAFS studies.[27] Furthermore, the formation of the MoO_2 phase is also seen by means of UV−vis spectroscopy. With respect to these studies and L_3-edge XANES, the intensity of the MoO_2 phase is less observed in the near-surface region than in the bulk. It is concluded that the reduction of Mo ions to form a MoO_2 phase is more effective in the bulk than in the near-surface region. This feature of the effect of reduction over Mo−Mg binary oxides is very similar to that on Mo−Sn binary oxides, as reported by Okamoto et al.[20]

In a previous report,[26] the metathesis reactivity for olefins is brought about for the reduced samples at around $x = 0.7$. These samples have small particles of the MoO_2 phase in the bulk.[27] As discussed above, the active species for metathesis reaction relates to the reduced Mo ions including the MoO_2 phase not only in the bulk but also in the near-surface region. The Mo ions in the near-surface region are reduced more difficulty than those in the bulk. However, the MoO_2 phase is stabilized in the near-surface region as a minor component. We suppose that these species act as an active center for metathesis, and the correlation between bulk and surface Mo ions relates to the stabilization of active species with low-valent Mo ions.

Acknowledgment. The X-ray absorption experiments at the Mo L-edge were supported by the Joint Studies Program (Proposal No. 6-841, 1994, and 7-542, 1995) of UVSOR of the Institute for Molecular Science. We thank Mr. Osamu Matsudo and Dr. Toyohiko Kinoshita (Institute for Molecular Science, Japan) for the assistance with XANES spectra measurements and helpful discussions. We acknowledge the invaluable indication of the reviewer about the penetration range of XANES spectra.

References and Notes

(1) Mol, J. C.; Moulijn, J. A. *Adv. Catal.* **1975**, *24*, 131.
(2) Gardin, D. J.; Lappert, M. F. *J. Chem. Soc., Chem. Commun.* **1972**, *927*, 927.
(3) Mol, J. C.; Moulijn, J. A. *Catal. Sci. Technol.* **1988**, *8*, 69.
(4) Rappe, A. K.; Goddard, W. A. *J. Am. Chem. Soc.* **1980**, *102*, 5114.
(5) Lombardo, E. A.; Houalla, M.; Hall, W. K. *J. Catal.* **1978**, *51*, 256.
(6) Gassman, P. G.; Johnson, T. H. *J. Am. Chem. Soc.* **1976**, *28*, 6055.
(7) Kazansky, V. B.; Shelimov, B. N.; Vikulov, K. A. In *Proceedings of the 10th International Congress on Catalysis*; Elsevier: Budapest, 1992; p 515.
(8) Vikulov, K. A.; Elev, I. V.; Shelimov, B. N.; Kazansky, V. B. *J. Mol. Catal.* **1989**, *55*, 126.
(9) Elev, I. V.; Shelimov, B. N.; Kazansky, V. A. *J. Catal.* **1988**, *113*, 229.
(10) Tanaka, K.; Miyahara, K.; Tanaka, K. In *Proceedings of the 7th International Congress Catalysis*; Elsevier: Tokyo, 1981; p 1318.
(11) Zhang, B.; Li, Y.; Lin, Q.; Jin, D. *J. Mol. Catal.* **1988**, *46*, 229.
(12) Anpo, M.; Kubokawa, Y. *J. Catal.* **1982**, *75*, 204.
(13) Anpo, M.; Kondo, M.; Kubokawa, Y.; Louis, C.; Che, M. *J. Chem. Soc., Faraday Trans. 1* **1988**, *84* (8), 2771.
(14) Llorente, J. M. M.; Rives, V.; Malet, P.; Gil-Llanbias, F. J. *J. Catal.* **1992**, *135*, 1.
(15) Deo, G.; Wachs, I. E. *J. Phys. Chem.* **1991**, *95*, 5889.
(16) Shimada, H.; Matsubayashi, N.; Sato, T.; Yoshimura, Y.; Nishiyama, A.; Kosugi, N.; Kuroda, H. *J. Catal.* **1992**, 746.
(17) Stampfl, S. R.; Chen, Y.; Dumesic, J. A.; Niu, C.; Hill, C. G., *J. Catal.* **1987**, *105*, 445.
(18) Moro-oka, Y.; Ueda, W. *Adv. Catal.* **1994**, *40*, 233.
(19) Glaeser, L. C.; Brazdil, J. F.; Hazle, M. A.; Mehicic, M.; Grasselli, R. K. *J. Chem. Soc., Faraday Trans. 1* **1985**, *81*, 2903.
(20) Okamoto, Y.; Oh-hiraki, K.; Imanaka, T.; Teranishi, S. *J. Catal.* **1981**, *71*, 99.
(21) Margolis, L. Y. *J. Catal.* **1971**, *21*, 93.
(22) Takita, Y.; Ozaki, A.; Morooka, Y. *J. Catal.* **1972**, *27*, 185.
(23) Morooka, Y.; Takita, Y.; Ozaki, A. *J. Catal.* **1971**, *23*, 183.
(24) Yun, Y.; Ueda, W.; Moro-oka, M. The 72nd Annual Meeting of the Catalysis Society of Japan, Nishinomiya, 1993.
(25) Tomenov, D. N.; Doroshenko, V. A.; Shapavolova, L. P.; Taranukha, O. M.; Lushnik, N. S. *Ukr. Khim. Zr.* **1981**, *74*, 93.
(26) Hasegawa, S.; Tanaka, T.; Kudo, M.; Mamada, H.; Hattori, H.; Yoshida, S. *Catal. Lett.* **1992**, *12*, 255.
(27) Aritani, H.; Tanaka, T.; Funabiki, T.; Yoshida, S.; Kudo, M.; Hasegawa, S. *J. Phys. Chem.* **1996**, *100*, 5440.
(28) Bare, S. R.; Mitchell, G. E.; Maj, J. J.; Vrieland, G. E.; Gland, J. L. *J. Phys. Chem.* **1993**, *97*, 6048.
(29) Teo, B. K.; Lee, P. A. *J. Am. Chem. Soc.* **1979**, *101*, 2815.
(30) Evans, J.; Frederick, W.; Mosselmans, W. *J. Phys. Chem.* **1991**, *95*, 9673.
(31) George, G. N.; Cleland, W. E., Jr.; Enemark, J. H.; Smith, B. E.; Kipke, C. A.; Roberts, S. A.; Cramer, S. P. *J. Am. Chem. Soc.* **1990**, *112*, 2541.
(32) Hedman, H.; Frank, P.; Gheller, S. F.; Roe, A. L.; Newton, W. E.; O., H. K. *J. Am. Chem. Soc.* **1988**, *110*, 3798.
(33) Hu, H.; Wachs, I. E.; Bare, S. R. *J. Phys. Chem.* **1995**, *99*, 10897.
(34) Chang, S.-C.; Leugers, M. A.; Bare, S. R. *J. Phys. Chem.* **1992**, *96*, 10358.
(35) Che, M.; Figueras, F.; Forisser, M.; McAtter, J.; Perrin, M.; Portefaix, J. L.; Praliaud, H. In *Proceedings of the 6th International Congress on Conference Catalysis*; Elsevier: London, 1976; p 261.
(36) Goodenough, J. B. In *4th Inernational Conference on Chemistry and Uses of Molybdenum*; Climax Molybdenum Co.: London, 1982; p 1.
(37) Sotani, N.; Kawamoto, Y.; Inui, M. *Mater. Res. Bull.* **1983**, *18*, 797.
(38) Sotani, N.; Eda, K.; Sadamatsu, M.; Takagi, S. *Bull. Chem. Soc. Jpn.* **1989**, *62*, 903.
(39) Erbil, A.; Cargill, G. S.; Frahm, R.; Boehme, R. F. *Phys. Rev. B* **1988**, *37*, 2450.
(40) Masure, D.; Chaquin, P.; Louis, C.; Che, M.; Fournier, M. *J. Catal.* **1989**, *119*, 415.
(41) Maksimovskaya, R. I.; Chumachenko, N. N. *Polyhedron* **1987**, *6*, 1813.
(42) Fedotov, M. A. *Bull. Acad. Sci. USSR, Div. Chem. Sci.* **1984**, 1070.
(43) Kihlborg, L. *Ark. Kemi.* **1963**, *21*, 357.
(44) Hibble, S. J.; Dickens, P. G. *Ber. Bunsen-Ges. Phys. Chem.* **1986**, *90*, 702.
(45) Sotani, N.; Eda, K.; Kunitomo, M. *J. Chem. Soc., Faraday Trans.* **1990**, *86* (9), 1583.
(46) Sotani, N.; Yoshida, N.; Yoshioka, Y.; Kishimoto, S. *Bull. Chem. Soc. Jpn.* **1985**, *58*, 1626.
(47) Thomas, D. M.; McCarron, E. M. III. *Mater. Res. Bull.* **1986**, *21*, 945.
(48) Beatham, N.; Orchard, A. F. *J. Electron. Spectrosc. Relat. Phenom.* **1979**, *16*, 77.
(49) Hughbanks, T.; Hoffmann, R. *J. Am. Chem. Soc.* **1983**, *105*, 1150.
(50) Fournier, M.; Louis, C.; Che, M.; Chaquin, P.; Masure, D. *J. Catal.* **1989**, *119*, 400.
(51) Prialiaud, H. In *2nd International Conference on Chemistry and Uses of Molybdenum*; Climax Molybdenum Co.: London, 1976; p 195.
(52) Massoth, F. E. *Adv. Catal.* **1978**, 265.
(53) Cotton, F.; Wilkinson, G. *Advances in Inorganic Chemistry (4th ed.)*; Interscience: New York, 1980; p 847.
(54) Weber, R. S. *J. Catal.* **1995**, *151*, 470.

JP9615464